Journal of Applied Mechanics and Technical Physics, Vol. 42, No. 5, pp. 748–756, 2001

ENTRANCE OF A BODY WITH A LIFTING FORCE AND A HEAT-CONDUCTING SURFACE INTO THE EARTH'S ATMOSPHERE

A. I. Borodin

UDC 519.86:533.6.011

The problem of gliding descent of a smooth blunted body possessing a lifting force and a heat-conducting surface in the Earth's atmosphere is solved. The descent trajectory is represented not only by the altitude and velocity as functions of the flight time but also by angles of attack and sideslip varying with time. Three-dimensional equations of a parabolized viscous shock layer for a multispecies mixture of gases are solved jointly with a three-dimensional equation of unsteady heat conduction in the solid phase.

Introduction. In an actual flight, because of intense interaction of the gas flow and the shell of a flying vehicle, the temperature of the body surface and the convective heat flux toward it are functions of the flight time. For this reason, it is necessary to consider the interrelated transfer processes in the gaseous and solid phases [1]. In addition, when bodies move in the atmosphere with high supersonic velocities, gas heating in the subsurface layer initiates various physicochemical processes, which should be taken into account to obtain a realistic physical flow pattern. Determination of heat-transfer characteristics on the surface of a descending body should be based on the solution of differential equations of external gas dynamics in multispecies reacting gas mixtures together with the heat-conduction equation in the protective shell of this body [2].

In the present paper, the dissociating air flow around spatial blunted bodies is considered within the framework of the parabolized viscous shock layer model, which is a modification of the general theory of the viscous shock layer [3] proposed initially for uniform gas flows [4, 5] and then for a multispecies mixture of gases [6]. Multispecies diffusion and homogeneous chemical reactions, including dissociation-recombination and exchange reactions, are considered. The generalized Rankine–Hugoniot conditions are set on the shock wave, and conditions taking into account heterogeneous catalytical reactions are imposed on the body surface. Viscous shock layer equations are solved jointly with the spatial equation of heat conduction inside the coating. The problem in such an adjoint formulation was numerically studied for the case of motion of an elliptic paraboloid along the reentry trajectory into the Earth's atmosphere.

Adjoint heat transfer within the framework of the viscous shock layer theory was previously taken into account in analysis of the flow around the stagnation point [7], axisymmetric flows [8], and spatial flows with a fixed angle of attack (there is a plane of symmetry in the flow) [9].

1. Formulation of the Problem. For a numerical solution of the problem of a hypersonic flow of a chemically nonequilibrium gas mixture around a blunted body at angles of attack and sideslip, we use a curved coordinate system x^i fitted to the body surface: the x^3 axis is directed along the normal to the body, and the x^1 and x^2 axes are located on the body surface. We write the equations of the spatial parabolized viscous shock layer, which describe the flow between the body surface and detached shock wave, taking into account nonequilibrium chemical reactions and multispecies diffusion and ignoring thermal diffusion, diffusion thermoeffect, and pressure diffusion, in dimensionless variables in the chosen coordinate system [6]:

$$D_\alpha(\rho u^\alpha \sqrt{g/g_{(\alpha\alpha)}}) + \sqrt{g}\, D_3(\rho u^3) = 0; \tag{1}$$

$$\rho(Du^\alpha + A^\alpha_{\beta\delta} u^\beta u^\delta) = -g^{\alpha\beta}\sqrt{g_{(\alpha\alpha)}}\, D_\beta P + D_3((\mu/\mathrm{Re}) D_3 u^\alpha); \tag{2}$$

Institute of Applied Mathematics and Mechanics, Tomsk State University, Tomsk 634050. Translated from Prikladnaya Mekhanika i Tekhnicheskaya Fizika, Vol. 42, No. 5, pp. 16–26, September–October, 2001. Original article submitted January 19, 2001.

 0021-8944/01/4205-0748 $25.00

$$D_3 D_\alpha P = -D_\alpha(\rho A^3_{\beta\delta} u^\beta u^\delta); \tag{3}$$

$$\rho(Du^3 + A^3_{\beta\delta} u^\beta u^\delta) = -D_3 P; \tag{4}$$

$$\rho c_p DT - 2D^* P = D_3\Big(\frac{\mu c_p}{\sigma \mathrm{Re}}\, D_3 T\Big) + \frac{\mu}{\mathrm{Re}}\, B_{\alpha\beta} D_3 u^\alpha D_3 u^\beta - D_3 T \sum_{i=1}^{N} c_{pi} I_i - \sum_{i=1}^{N} h_i \dot{w}_i; \tag{5}$$

$$\rho D c_i + D_3 I_i = \dot{w}_i \quad (i = 1, \ldots, N-1); \tag{6}$$

$$P = \rho T R \sum_{i=1}^{N} \frac{c_i}{m_i}, \qquad c_p = \sum_{i=1}^{N} c_{pi} c_i; \tag{7}$$

$$\sum_{i=1}^{N} c_i = 1, \qquad \sum_{i=1}^{N} I_i = 0. \tag{8}$$

Here $D_i \equiv \partial/\partial x^i$, $D^* \equiv (u^\alpha/\sqrt{g_{(\alpha\alpha)}})D_\alpha$, $D \equiv D^* + u^3 D_3$, and $\mathrm{Re} = \rho_\infty V_\infty L/\mu(T_0)$ ($T_0 = 10^4$ K).

System (1)–(8) is closed by the Stefan–Maxwell relations

$$\begin{gathered}
\sum_{j=1}^{N-1} a_{ij} I_j = -\frac{\mu}{\mathrm{ReSc}_{lN}} \sum_{j=1}^{N-1} b_{ij} D_3 c_j, \quad i = 1, \ldots, N-1\ , \\
a_{ij} = -a^*_{ij} c_i, \qquad b_{ij} = -b^*_j c_i \qquad (i \neq j), \\
a_{ii} = \frac{\mathrm{Sc}_{iN}}{\mathrm{Sc}_{lN}} + \sum_{j=1,\ j\neq i}^{N-1} a^*_{ij} c_j, \qquad b_{ii} = 1 + \sum_{j=1,\ j\neq i}^{N-1} b^*_j c_j, \\
a^*_{ij} = \frac{m_N}{m_j}\frac{\mathrm{Sc}_{ij}}{\mathrm{Sc}_{lN}} - \frac{\mathrm{Sc}_{iN}}{\mathrm{Sc}_{lN}}, \qquad b^*_j = \frac{m_N}{m_j} - 1, \qquad \mathrm{Sc}_{ij} = \frac{\mu}{\rho D_{ij}}.
\end{gathered} \tag{9}$$

Here $V_\infty u^i$ are the physical components of the velocity vector along the corresponding coordinate axes, $\rho_\infty V^2_\infty P$, $\rho_\infty \rho$, and $T_0 T$ are, respectively, the pressure, density, and temperature of the gas mixture consisting of N chemical components, $\mu(T_0)\mu$, $(V^2_\infty/(2T_0))c_p$, and σ are the viscosity, specific heat capacity, and Prandtl number, respectively, c_i, m_i, $0.5V^2_\infty h_i$, $(V_\infty/(2T_0))c_{pi}$, $V_\infty \rho_\infty I_i$, and $V_\infty \rho_\infty \dot{w}_i/L$ are, respectively, the mass concentration, molecular weight, specific enthalpy, specific heat capacity, normal component of the diffusion-flux vector, and mass-formation rate of the ith component as a result of chemical reactions, D_{ij} and Sc_{ij} are binary coefficients of diffusion and Schmidt number, respectively, $R_G = V^2_\infty R/T_0$ is the universal gas constant, $g_{\alpha\beta}$ and $g^{\alpha\beta}$ are the covariant and contravariant components of the first quadratic form of the body surface, $g = g_{11}g_{22} - g^2_{12}$, and A^k_{ij} are known functions of the shape of the body [10]. Summation is performed over repeated subscripts that are not enclosed in brackets. The Latin subscripts take values 1, 2, and 3 (except for specially indicated cases); the Greek sub- and superscripts equal 1 or 2. All linear dimensions are normalized to the characteristic linear size L. The subscripts w, ∞, and s refer to quantities on the body surface, in the free stream, and behind the shock wave.

The equations of the viscous shock layer are solved jointly with the heat-conduction equation in the same curved coordinate system x^i:

$$\frac{\partial T_B}{\partial t} = \frac{æ}{\sqrt{g}}\Big(D_1\,\frac{g_{22}D_1T_B - g_{12}D_2T_B}{\sqrt{g}} + D_2\,\frac{g_{11}D_2T_B - g_{12}D_1T_B}{\sqrt{g}} + D_3\,\frac{D_3T_B}{\sqrt{g}}\Big). \tag{10}$$

Here $æ = \lambda_B t^*/(\rho_B c_{pB} L^2)$ and t is the time normalized to the characteristic flight time t^*; the subscript B refers to the parameters of the solid phase (body).

The system of differential equations of the viscous shock layer (1)–(6) and the heat-conduction equation (10) are solved under the following boundary conditions:

— on the shock wave,

$$x^3 = x_s^3(x^1, x^2): \quad \rho(u^3 - D^* x^3) = u_\infty^3, \quad u_\infty^3(u^\alpha - u_\infty^\alpha) = (\mu/\mathrm{Re}) D_3 u^\alpha,$$
$$P = (u_\infty^3)^2, \quad u_\infty^3(c_i - c_{i\infty}) + I_i = 0 \quad (i = 1, \ldots, N-1),$$
$$\frac{\mu c_p}{\sigma u_\infty^3 \mathrm{Re}} D_3 T = \sum_{i=1}^{N} c_{i\infty}(h_i - h_{i\infty}) - (u_\infty^3)^2 - B_{\alpha\beta}(u^\alpha - u_\infty^\alpha)(u^\beta - u_\infty^\beta); \tag{11}$$

— at the interface between the solid and gaseous phases,

$$x^3 = 0: \quad u^i = 0, \quad I_i = \dot{r}_i \quad (i = 1, \ldots, N-1), \quad T = T_B,$$
$$\frac{\mu c_p}{\sigma \mathrm{Re}} D_3 T - \sum_{i=1}^{N} h_i I_i = \Lambda D_3 T_B + \Gamma T_B^4; \tag{12}$$

— at the inner side of the coating,

$$x^3 = -l/L: \quad D_3 T_B = 0. \tag{13}$$

Here $\rho_\infty V_\infty \dot{r}_i$ is the rate of formation of the ith component due to heterogeneous reactions, $\Lambda = \lambda_B/(\rho_\infty V_\infty c_{p\infty} L)$, $\Gamma = 2\varepsilon_B \sigma_B T_0^4/(\rho_\infty V_\infty^3)$, ε_B is the emissivity of the surface, σ_B is the Stefan–Boltzmann constant, and l is the coating thickness.

The initial condition for Eq. (10) is the initial temperature of the shell. The dissociating air in the shock layer is represented as a perfect mixture of five chemical components (O_2, N_2, NO, O, and N), in which dissociation–recombination and exchange reactions proceed. The dependences of the rate constants of direct and reverse reactions on temperature were determined in accordance with [11]. The transfer coefficients and thermodynamic functions were calculated by formulas from [12–16].

The atmosphere is assumed to be isothermal and have a density distribution ρ_∞ [g/cm^3] over the height H [km]: $\rho_\infty = 1.225 \cdot 10^{-3} \exp(-0.142H)$. It is assumed that heterogeneous catalytical reactions are first-order reactions: $\dot{r}_i = -\rho k_{wi} c_i$ ($i \equiv$ O, N, and NO), where $V_\infty k_{wi}$ is the rate constant of heterogeneous recombination. Two models of catalytical interaction between the gas and the solid surface were considered: 1) $k_{wi} = 0$ (neutral surface); 2) $k_{wi} = \infty$ (ideally catalytical surface).

2. Method of the Solution of Viscous Shock Layer Equations. To find the numerical solution of the problem in the gas phase on the body surface, we choose a polar coordinate system with the origin at the stagnation point [17], which is degenerate at this point. At the stagnation point, the normal to the body surface coincides with the free-stream direction, which is completely determined by the angles of attack α and sideslip β. One family of coordinate lines ($x^1 = \mathrm{const}$) consists of concentric "circles," and the other ($x^2 = \mathrm{const}$) is a bunch of "beams" with the center in the origin.

Taking into account the special features of the chosen coordinate system on the surface, we pass to new variables

$$\xi^\alpha = x^\alpha, \qquad \zeta = \frac{1}{\Delta} \int_0^{x^3} \rho \, dx^3, \qquad \Delta = \Delta(\xi^1, \xi^2) = \int_0^{x_s^3} \rho \, dx^3,$$

$$\frac{\partial f_\alpha}{\partial \zeta} = \frac{u^\alpha}{u_*^\alpha}, \qquad \theta = \frac{T}{T_*}, \qquad u_*^1 = u_\infty^1, \quad u_*^2 = \xi^1, \qquad T_* = \frac{(u_\infty^3)^2}{2},$$

$$\rho u^3 \sqrt{g} = -\frac{\partial}{\partial \xi^\alpha}(\psi_*^{(\alpha)} f_\alpha) - \psi_*^{(\alpha)} \frac{\partial f_\alpha}{\partial \zeta} \frac{\partial \zeta}{\partial x^\alpha},$$

$$\psi_*^\alpha = \Delta u_*^\alpha \sqrt{\frac{g}{g_{(\alpha\alpha)}}}, \qquad P_\alpha = \frac{1}{(\xi^1)^\alpha} \frac{\partial P}{\partial \xi^\alpha}, \qquad X_i = \frac{I_i}{\Delta} \quad (i = 1, \ldots, N),$$

which allows us to resolve singularities at the stagnation point.

In the new variables, the continuity equation (1) is satisfied identically; the entire system of differential equations (2)–(8) with the boundary conditions (11) and (12) in these variables can be found in [6].

The Stefan–Maxwell relations are written in the form [18]

$$X_i = \alpha_i \frac{\partial c_i}{\partial \zeta} + \beta_i c_i \quad (i = 1, \ldots, N-1). \tag{14}$$

To determine the flux X_i, the corresponding continuity equation for the ith component is integrated; to calculate the concentration c_i, this equation with substitution of X_i from Eq. (14) is used. This approach allows one to find the unknown concentrations of the gases in the mixture without prior resolution of the Stefan–Boltzmann relations with respect to diffusion fluxes.

Thus, the resultant system of equations that describes the flow of the mixture in the shock layer contains two third-order equations along the transverse coordinate ζ with respect to the stream functions f_α, a second-order equation for the temperature θ, a second-order equation for the x^3 coordinate (which is a consequence of the momentum equation in projection onto the normal to the body surface, continuity equation, and equation of state), two first-order equations for longitudinal components of the pressure gradient P_α, $N-1$ first-order equations for diffuse fluxes X_i, and $N-1$ second-order equations for concentrations c_i.

The normal component of the velocity vector u^3 and the density ρ are determined by the formulas

$$u^3 = -A \frac{\partial x^3}{\partial \zeta} + (\xi^1)^{2-\alpha} \frac{\partial f_\alpha}{\partial \zeta} \frac{\partial x^3}{\partial \xi^\alpha}, \qquad \rho = \frac{\Delta \xi^1}{\sqrt{g}} \Big(\frac{\partial x^3}{\partial \zeta} \Big)^{-1}.$$

For numerical integration of the second- and third-order differential equations with respect to the transverse coordinate ζ, an implicit finite-difference scheme was used, which had an order of approximation $O(\delta\xi^1) + O(\delta\xi^2)^2 + O(\delta\zeta)^4$. This scheme is a generalization of the scheme of [19] to the three-dimensional case and employs a variable step along the ζ coordinate. In the convective operator, the derivatives with respect to the marching coordinate ξ^1 are replaced by upstream differences, and the derivatives with respect to the circumferential coordinate ξ^2 are approximated by central differences on the basis of a solution obtained at the previous iteration on the current "circumference" $\xi^1 + \delta\xi^1 = \text{const}$.

The first-order equations are integrated by Simpson's method with a fourth-order accuracy in terms of ζ.

The value of $\Delta(\xi^1, \xi^2)$ is determined after the calculation of the entire "circumference" at each iteration by the method of cyclic sweep [20] and, thus, is a matching function of the solutions obtained at all computational points of the current "circumference."

Since the coordinate system (ξ^1, ξ^2) introduced on the body surface degenerates at the stagnation point, a non-degenerate curved coordinate system was used to solve the initial equations at this point. The solution obtained was then recalculated to the coordinate system (ξ^1, ξ^2, ζ) using algebraic formulas from [17] and was assumed to be the initial solution for calculation of the entire domain.

To increase the calculation accuracy at high Reynolds numbers, a difference grid nonuniform along the ζ coordinate (condensing toward the body surface) was used. In this case, to identify a thin boundary layer near the body surface, an iterative process of grid adaptation was used, which ensured an approximately uniform increment of the sought functions at each step along the ζ coordinate in solving the viscous shock layer equations at the stagnation point. The distribution of nodes along ζ obtained at the stagnation point was used for all other calculation nodes of the wetted surface.

3. Method of the Solution of the Heat-Conduction Equation. In the numerical solution of the problem of heat propagation inside the body, we used the same coordinate system as in calculations of the gas phase, but the system was fixed and had the origin in the center of the body (at zero incidence, the coordinate systems along the surface for the gas phase and heat propagation inside the body coincide). This choice of the coordinate system is conditioned by the fact that the domains of integration along the body surface coincide; in addition, Eq. (10) is significantly simplified due to the orthogonality of the coordinate system ($g_{12} = 0$). Taking into account the special features at the origin, the heat-conduction equation acquired the form

$$\frac{1}{æ} \frac{\sqrt{g}}{\xi} \frac{\partial T}{\partial t} - \frac{\partial}{\partial \xi} \Big(\frac{g_{22}}{\sqrt{g}} \Big) \frac{1}{\xi} \frac{\partial T}{\partial \xi} - \frac{g_{22}}{\xi \sqrt{g}} \frac{\partial^2 T}{\partial \xi^2} - \frac{\partial}{\partial \eta} \Big(\frac{g_{11} \xi}{\sqrt{g}} \Big) \frac{1}{\xi^2} \frac{\partial T}{\partial \eta} - \frac{\xi g_{11}}{\sqrt{g}} \frac{1}{\xi^2} \frac{\partial^2 T}{\partial \eta^2} - \frac{\sqrt{g}}{\xi} \frac{\partial^2 T}{\partial \zeta^2} = 0. \tag{15}$$

The notations $\xi \equiv x^1$, $\eta \equiv x^2$, $\zeta \equiv x^3$, and $T \equiv T_B$ are used here for convenience. In the origin ($\xi = 0$), this equation degenerates into

$$\frac{1}{æ}\,\frac{\sqrt{g}}{\xi}\,\frac{\partial T}{\partial t}-\Big(\frac{\partial}{\partial\xi}\Big(\frac{g_{22}}{\sqrt{g}}\Big)+\frac{g_{22}}{\xi\sqrt{g}}\Big)\frac{\partial^2 T}{\partial\xi^2}-\frac{1}{2}\,\frac{\partial}{\partial\eta}\Big(\frac{\xi g_{11}}{\sqrt{g}}\Big)\frac{\partial}{\partial\eta}\Big(\frac{\partial^2 T}{\partial\xi^2}\Big)$$

$$-\frac{1}{2}\,\frac{\xi g_{11}}{\sqrt{g}}\,\frac{\partial^2}{\partial\eta^2}\Big(\frac{\partial^2 T}{\partial\xi^2}\Big)-\frac{\sqrt{g}}{\xi}\,\frac{\partial^2 T}{\partial\zeta^2}=0. \tag{16}$$

It follows from analysis of Eq. (16) that, for $\xi = 0$, the derivatives $\partial T/\partial\xi$ and $\partial^2 T/\partial\xi^2$ are equal to zero.

The heat-conduction equation (15) was solved using an implicit three-step scheme of the method of alternating directions, which was proposed by Douglas [21] (see also [22]). The scheme has the order of accuracy $O(\delta t^2, \delta\xi^2, \delta\eta^2, \delta\zeta^2)$ and is unconditionally stable.

At the first step, all derivative with respect to ξ in Eq. (15) were approximated by central differences, and derivatives along two remaining directions were calculated previously. At both boundaries of the domain of integration, zero second derivatives were prescribed along the marching coordinate ξ. The solution of the thus-obtained system of three-point equations with respect to the temperature T was found by the sweep method [20]; after that, the derivatives $\partial T/\partial\xi$ and $\partial^2 T/\partial\xi^2$ were calculated using the same central differences.

At the second step, the derivatives with respect to η were approximated by central differences, the condition of periodicity of temperature along this variable being taken into account. The derivatives with respect to ξ and ζ are known. The resultant system of three-point equations with respect to the function T/ξ^2 (which is important for stability of sweep in the vicinity of the origin) was solved by the method of cyclic sweep [20]. Based on the temperature found, the derivatives $\partial T/\partial\eta$ and $\partial^2 T/\partial\eta^2$ were calculated.

At the third step, the temperature was finally determined using the same implicit finite-difference scheme of the fourth-order approximation with respect to the variable ζ [19] but on a constant uniform grid with known derivatives along two remaining spatial variables and specified first derivatives with respect to ζ at the boundaries.

Owing to the adopted assumption on quasi-steadiness of the processes in the gas phase, the generic algorithm of solving the adjoint problem is as follows: for a surface temperature known at the initial time, all parameters of the flow of the mixture are calculated with a given accuracy within the entire region between the body surface and the shock-wave surface. After that, the body-temperature gradient along the normal coordinate is determined from the heat-flux balance equation at the interface between the gaseous and solid media; this gradient is the boundary condition for the heat-conduction equation. When the temperature field inside the shell with a new value of temperature is calculated, the parameters in the gaseous medium are determined. The process is repeated, and the input parameters of the flow in the viscous shock layer (height H, flight velocity V_∞, angles of attack and sideslip, and, as a consequence, the flow parameters at infinity) are calculated for the next current point of the trajectory.

The special feature of the numerical method proposed for solving the adjoint problem is the fact that its implementation does not require the presence of planes of symmetry in the flow (therefore, it is possible to perform calculations for the general case of the flow around bodies with heat-conducting surfaces at angles of attack and sideslip), and the calculation of friction and heat-transfer coefficients on the body surface does not require numerical differentiation of velocity and temperature profiles across the shock layer. The calculations showed that this method is stable, economic and allows solving the adjoint problem in a wide range of governing parameters corresponding to a given flight trajectory.

4. Results. The reentry body was assumed to be an elliptic paraboloid, which is described by the following equation in the Cartesian coordinate system:

$$2z = (x/b)^2 + (y/c)^2, \qquad b = 1, \quad c = 1.5811. \tag{17}$$

The ratio of the main curvatures at the apex of this paraboloid is $k = 0.4$. The characteristic linear size in the problem is the least radius of the main curvatures at this point $L = 0.5$ m. The emissivity of the surface is $\varepsilon_B = 0.85$. The materials used for the heat-protective coating were graphite [$\rho_B c_{pB} = 1.6$ J/(K · cm^3) and $\lambda_B = 0.88$ W/(K · cm)] and quartz [$\rho_B c_{pB} = 1.77$ J/(K · cm^3) and $\lambda_B = 0.046$ W/(K · cm)]. The initial temperature of the coating was 300 K.

To confirm the reliability of the results described below, we solved the problem of the flow around this paraboloid under conditions of its motion along the reentry trajectory into the Earth's atmosphere, which was borrowed from [23]. The temperatures of the heat-conducting surface (graphite coating was 2 cm thick, and heat overflow along the coating was neglected) at the paraboloid apex, which were obtained in the present work, coincided with data presented in [9] for both models of heterogeneous catalytical reactions. Under the same conditions, the

TABLE 1

Number of control point	H, km	V, m/sec	t, sec	α, deg	β, deg
1	122.0	7810	0	34	30
2	99.7	7840	190	34	24
3	76.1	7680	430	34	70
4	65.3	6240	900	32	53
5	48.4	2724	1470	30	10
6	46.8	2440	1525	30	17
7	27.4	985	1790	15	29
8	21.8	463	1905	10	−10
9	21.4	454	1909	10	−10

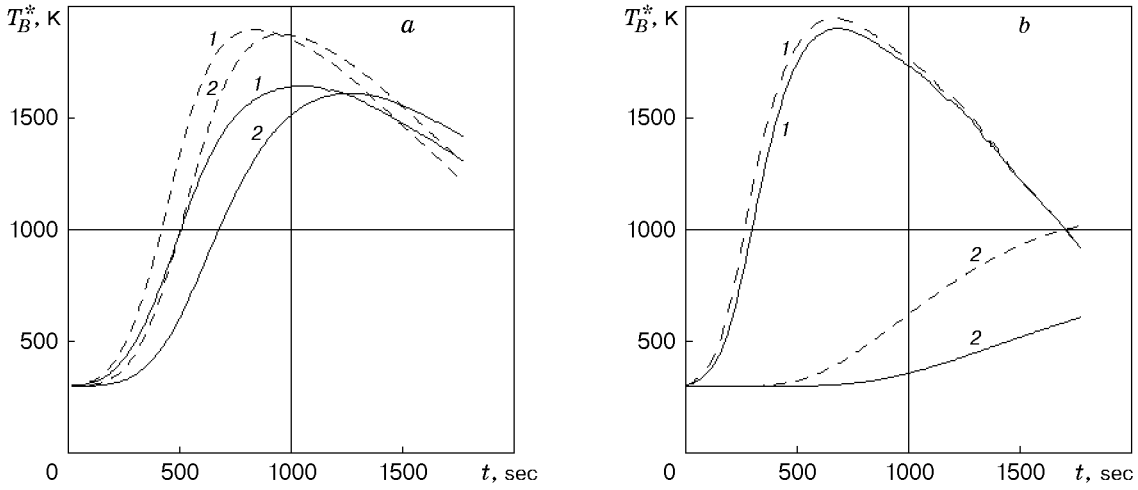

Fig. 1

effect of the step of integration in time was investigated, and it was found that the numerical results almost coincide for $\delta t = 10$ and 1 sec. In all variants described below, the time step was 10 sec.

In the present work, we considered the descent of paraboloid (17) along the trajectory borrowed from [24]; its parameters are listed in Table 1.

The computational domain is a space enclosed between the shock-wave surface, the internal surface of the paraboloid shell, and the surface formed by the normals outgoing from the paraboloid cross section by the plane $z = 0.8$. This plane is chosen so that the stagnation point is inside the computational domain along the entire trajectory (i.e., for given α and β). Thus, the calculation of the flow of a multispecies mixture near the surface of an elliptic paraboloid in the chosen curved coordinate system begins from the stagnation point with the coordinate $\xi^1 = 0$ and ends in a given cross section that coincides with the coordinate line $\xi^1 = 1$; and the solution of the heat-conduction equation in the shell lies in the coordinate system (ξ, η, ζ), where $\xi = 0$ corresponds to the paraboloid apex, and the boundary $\xi = 1$ on the body surface coincides with the above-mentioned coordinate line $\xi^1 = 1$.

The purpose of the present numerical experiment is to evaluate the influence of heat overflow in longitudinal directions on heat-transfer characteristics for different materials of the heat-protective coating.

We consider the case, where the body is exposed to a counterflow at zero incidence. Then, the problem has two planes of symmetry, which coincide with the planes of symmetry of the paraboloid itself, and the curved coordinate systems on the body surface for the gaseous (ξ^1, ξ^2) and solid (ξ, η) phases coincide. Therefore, there is no need in interpolation of the boundary conditions from one difference grid to the other. This simplification of the problem allows also a significant decrease in the computation time. Calculation results for an ideally catalytical surface (model 2) are given below. In this case, as is shown by calculations and as follows from [9], all the results may be considered as the upper estimates for different heterogeneous catalytical reactions.

Figure 1 shows the temperature at the stagnation point at the outer (curves 1) and inner (curves 2) surfaces of the protective coating as a function of the flight time for graphite (Fig. 1a) and quartz (Fig. 1b) coatings 10 cm thick. The dashed and solid curves correspond to calculations performed with longitudinal heat overflow ignored and taken into account, respectively. For the graphite coating, the character of all dependences is similar: a clear

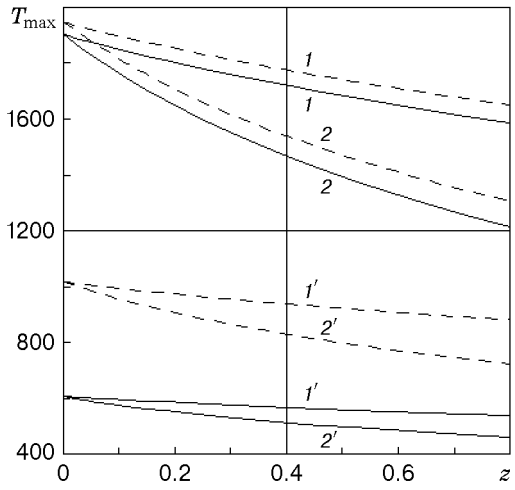

Fig. 2

maximum is observed, which is shifted in time and decreases by 250 K if heat overflow is taken into account. For the quartz coating, the picture is different. The dependence of the temperature of the outer side of the shell in both cases have maxima at the same point of the trajectory ($H = 67.5$ km and $V = 7150$ m/sec) with a difference of 35 K. At the same time, the temperature of the inner surface is a monotonically increasing function, and the influence of the heat-overflow process in longitudinal directions is more significant (the difference in temperature is greater than 400 K).

We introduce the notion of the maximum temperature of the heat-protective shell of the body during the flight time t_k: $T_{\max} = \max\limits_{0 \leqslant t \leqslant t_k} T_B(t, \xi, \eta, \zeta)$. Figure 2 shows the distribution of the maximum temperature of the outer (curves 1 and 2) and inner (curves $1'$ and $2'$) surfaces of the heat-protective quartz shell ($l = 10$ cm) during 1760 sec of motion of the paraboloid along a given trajectory with respect to the z coordinate along the planes of symmetry [$x = 0$ (curves 1 and $1'$) and $y = 0$ (curves 2 and $2'$)]. As in Fig. 1, the solid and dashed cures correspond to calculations with heat overflow along the body surface being taken into account and ignored, respectively. For all the distributions, the maximum is at the stagnation point (paraboloid apex). As in the problem for the stagnation point, the neglect of heat overflow in the longitudinal and circumferential directions leads to overprediction of the surface temperature in the entire computational domain.

We consider a more complicated problem — trajectorial motion of the paraboloid with regard for angles of attack and sideslip varying with time (see Table 1). We consider a quartz shell 10 cm thick. In this case, there is no symmetry in the problem, and the stagnation point changes its position on the body surface with changing angles α and β. The essentially three-dimensional character of the problem becomes more complicated if heat overflow along the longitudinal directions in the heat-conducting shell is taken into account.

The isolines of the surface temperature of the paraboloid (in Kelvin) in the (x, y) plane at different times of descent along the trajectory are plotted in Fig. 3. The diverging "beams" are the coordinate lines $\xi^2 = 0.5\pi k$ ($k = 0, \ldots, 3$), the point of their intersection ($\xi^1 = 0$) is the stagnation point, and the ellipse is the boundary of the computational domain ($\xi^1 = 1$, i.e., $z = 0.8$). The paraboloid apex with the coordinates $(0, 0)$ is located at the center of the ellipse. It is seen in Fig. 3 that the stagnation point is in the zone of elevated temperatures, though it is not the point of the maximum surface temperature. The zone itself is shifted over the body surface. Its shape and temperature change thereby.

Figure 4 shows the distribution of the limiting surface temperature of the paraboloid $T_{\max}$ reached during 1560 sec of flight for the cases where heat overflow along the body is taken into account (Fig. 4a) and where the heat propagates only in the direction normal to the surface (Fig. 4b). It is seen that the zone with temperatures higher than 1600 K is significantly smaller in the first case. The region in Fig. 4a with $T > 1400$ K was formed at $t = 1070$ sec and the region with $T < 1400$ K was formed at $t = 1300$ sec.

Figure 5 shows the distribution of the limiting temperature $T_{\max}$ of the inner surface of the shell for the same time and the same conditions as in Fig. 4. In Fig. 5, the influence of longitudinal heat overflow is even more pronounced: the positions of the zones of elevated temperatures do not coincide. In addition, the maximum

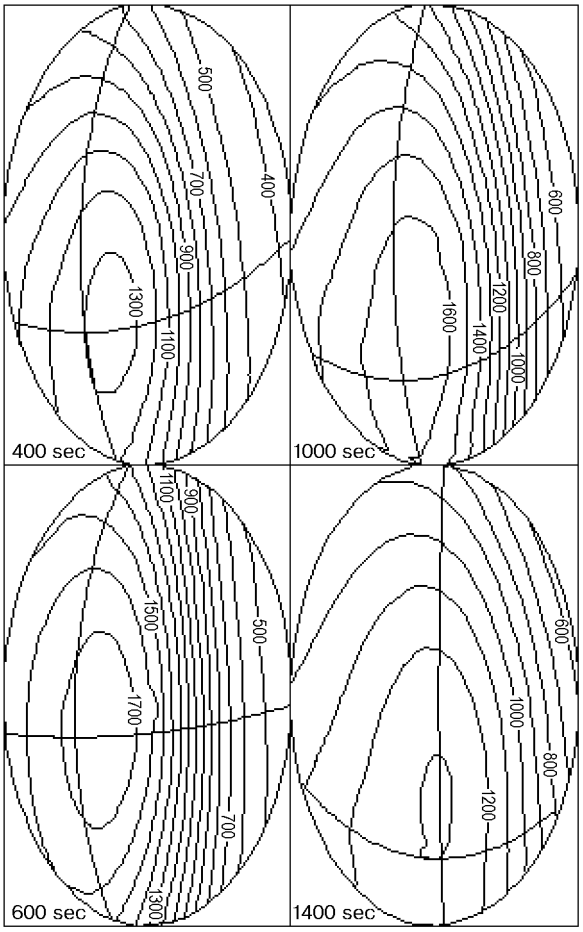

Fig. 3

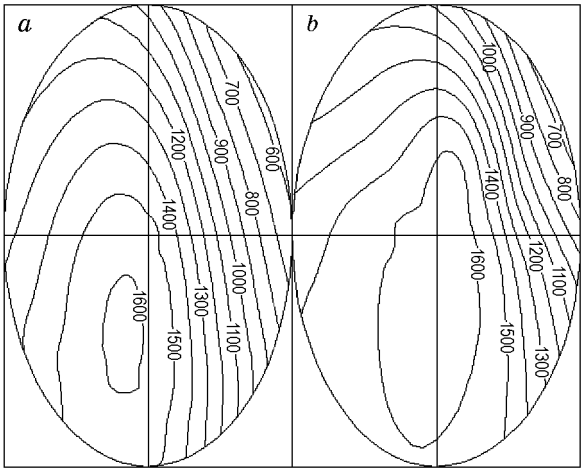

Fig. 4

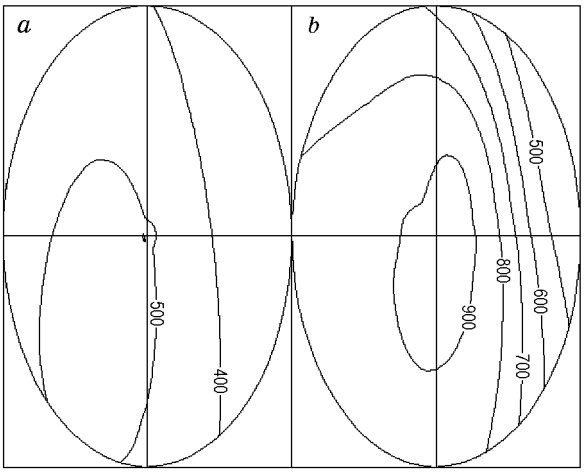

Fig. 5

temperature in Fig. 5a does not exceed 525 K, whereas $T_{\max} > 900$ K and the temperature is higher than 500 K almost within the entire zone in Fig. 5b. In contrast to the distribution of the maximum temperature of the outer surface of the shell, the pattern shown in Fig. 5 has been formed by the last moment of the flight time considered in the present work.

On the basis of numerous calculations and results presented in this work, we may conclude that taking into account of the lift-to-drag ratio of the descending vehicle and three-dimensional processes of heat propagation in its protective shell changes significantly the distribution of heat loads on the protected surface of the body, which should be taken into account in designing reentry vehicles.

This work was supported by the Russian Foundation for Fundamental Research (Grant No. 98-01-00298).

REFERENCES

1. Yu. V. Polezhaev and F. B. Yurevich, *Heat Protection* [in Russian], Énergiya, Moscow (1976).
2. A. V. Lykov, *Heat-Conduction Theory* [in Russian], Vysshaya Shkola, Moscow (1967).
3. R. T. Davis, "Numerical solution of the hypersonic viscous shock layer equations," *AIAA J.*, **8**, No. 5, 843–851 (1970).
4. A. I. Borodin and S. V. Peigin, "Spatial flow around blunted bodies within the framework of the parabolized viscous shock layer model," *Mat. Model.*, **5**, No. 1, 16–25 (1993).
5. A. I. Borodin and S. V. Peigin, "Parabolized viscous shock layer model in studying spatial hypersonic viscous gas flow around bodies," *Teplofiz. Vys. Temp.*, **31**, No. 6, 925–933 (1993).

6. A. I. Borodin, V. Yu. Kazakov, and S. V. Peigin, "Simulation of multispecies, chemically nonequilibrium flows within the framework of the parabolized spatial viscous shock layer model," *Mat. Model.*, **8**, No. 10, 3–14 (1996).
7. V. I. Zinchenko and S. I. Pyrkh, "Nonequilibrium viscous shock layer in the vicinity of the stagnation point with regard for adjoint heat transfer," *Prikl. Mekh. Tekh. Fiz.*, No. 3, 108–114 (1979).
8. V. I. Zinchenko and S. I. Pyrkh, "Calculation of a nonequilibrium viscous shock layer with regard for adjoint heat transfer," *Izv. Akad. Nauk SSSR, Mekh. Zhidk. Gaza*, No. 2, 146–153 (1984).
9. É. A. Gershbein, V. G. Krupa, and V. S. Shchelin, "Spatial, chemically nonequilibrium viscous shock layer on a catalytical surface with regard for adjoint heat transfer," *Izv. Akad. Nauk SSSR, Mekh. Zhidk. Gaza*, No. 6, 140–146 (1985).
10. Yu. D. Shevelev, *Three-Dimensional Problems of the Laminar Boundary-Layer Theory* [in Russian], Nauka, Moscow (1977).
11. E. W. Miner and C. H. Lewis, "Hypersonic ionizing air viscous shock-layer flows over nonanalytic blunt bodies," Report NASA No. 2550 (1975).
12. C. R. Wilke, "A viscosity equation of gas mixtures," *J. Chem. Phys.*, **18**, No. 4, 517–519 (1959).
13. E. A. Mason and S. C. Saxena, "Approximate formula for the thermal conductivity of gas mixtures," *Phys. Fluids*, **1**, No. 5, 361–369 (1958).
14. R. A. Svehla, "Estimated viscosities and thermal conductivities of gases at high temperatures," Report NASA No. R-132 (1962).
15. J. O. Hirchfelder, C. Curtiss, and R. Bird, *Molecular Theory of Gases and Liquids*, John Wiley and Sons, New York (1954).
16. L. V. Gurvich, I. V. Veits, V. A. Medvedev, et al., *Thermodynamic Properties of Individual Substances: Handbook* [in Russian], Vol. 1, Book 2, Nauka, Moscow (1978).
17. A. I. Borodin and S. V. Peigin, "Spatial thin viscous shock layer in the absence of planes of symmetry in the flow," *Izv. Akad. Nauk SSSR, Mekh. Zhidk. Gaza*, No. 2, 150–158 (1989).
18. É. A. Gershbein, "Laminar multi-species boundary layer at high injections," *Izv. Akad. Nauk SSSR, Mekh. Zhidk. Gaza*, No. 1, 64–73 (1970).
19. I. V. Petukhov, "Numerical calculation of two-dimensional flows in the boundary layer," in: *Numerical Methods of Solving Differential and Integral Equations and Quadrature Formulas* [in Russian], Nauka, Moscow (1964), pp. 305–325.
20. A. A. Samarskii and E. S. Nikolaev, *Methods of Solution of Grid Equations* [in Russian], Nauka, Moscow (1978).
21. J. Douglas, "Alternating direction methods for three space variables," *Numer. Math.*, **4**, 41–63 (1962).
22. P. J. Roache, *Computational Fluid Mechanics*, Hermosa, Albuquerque (1976).
23. R. V. Masek, D. Hender, and J. A. Forney, "Evaluation of aerodynamic uncertainties for space shuttle," AIAA Paper No. 737 (1973).
24. *Astronautics and Rocket Dynamics: Book of Abstracts*, No. 34, VINITI, Moscow (1974).